

Radio Halos From Simulations And Hadronic Models I: The Coma cluster

J. Donnert¹, K. Dolag¹, G. Brunetti², R. Cassano², A. Bonafede^{2,3}

¹Max Planck Institute for Astrophysics, P.O. Box 1317, D-85741 Garching, Germany

²INAF Istituto di Radioastronomia, via P. Gobetti 101, I-40129 Bologna, Italy

³Università di Bologna, Dip. di Astronomia, via Ranzani 1, I-40126 Bologna, Italy

Accepted ???. Received ???; in original form ???

ABSTRACT

We use the results from a constrained, cosmological MHD simulation of the Local Universe to predict the radio halo and the gamma-ray flux from the Coma cluster and compare it to current observations. The simulated magnetic field within the Coma cluster is the result of turbulent amplification of the magnetic field during build-up of the cluster. The magnetic seed field originates from star-burst driven, galactic outflows. The synchrotron emission is calculated assuming a hadronic model. We follow four approaches with different distributions for the cosmic-ray proton (CRp) population within galaxy clusters. The radial profile the radio halo can only be reproduced with a radially increasing energy fraction within the cosmic ray proton population, reaching $>100\%$ of the thermal energy content at $\approx 1\text{Mpc}$, e.g. the edge of the radio emitting region. Additionally the spectral steepening of the observed radio halo in Coma cannot be reproduced, even when accounting for the negative flux from the thermal SZ effect at high frequencies. Therefore the hadronic models are disfavored from present analysis. The emission of γ -rays expected from our simulated coma is still below the current observational limits (by a factor of ~ 6) but would be detectable in the near future.

Key words: galaxies:clusters:individual:Coma, intergalactic medium

1 INTRODUCTION

Galaxy clusters are the largest gravitationally bound objects in the Universe. The thermal gas, which forms the dominant component in the Intra-Cluster-Medium (ICM), is mixed with magnetic fields and relativistic particles, as seen by radio observations that detected Mpc-sized diffuse radio sources in a fraction of X-ray luminous galaxy clusters in the merging phase (e.g. Feretti 2003; Ferrari et al. 2008). A fraction of the energy dissipated during cluster mergers may be channelled into the amplification of the magnetic fields (e.g. Dolag et al. 2002; Subramanian et al. 2006) and into the acceleration of relativistic, primary electrons (CRE) and protons (CRp) via shocks and turbulence (Ensslin et al. 1998; Blasi 2001; Brunetti & Lazarian 2007). CRp have long life-times and remain confined within clusters for a Hubble time (e.g. Blasi et al. 2007, and ref. therein). Consequently they are expected to be the dominant non-thermal particle component in the ICM and to generate secondary particles through collisions with thermal protons. Primary and secondary particles in the ICM are expected to produce a complex emission spectrum from radio to γ -rays (see Petrosian et al. 2008; Brunetti 2008; Cassano 2009, for recent reviews).

Only upper limits to the γ -ray emission from clusters have been obtained so far (Reimer et al. 2003; Aharonian et al. 2009), although the FERMI telescope will shortly provide the chance to obtain the first γ -ray detections of clusters and to put stringent con-

straints to the energy density of the CRp. Future deep observations with high energy Cherenkov arrays are expected to provide complementary constraints. Most importantly, in a few years the Low Frequency Array (LOFAR) and the Long Wavelength Array (LWA) will observe clusters at low radio frequencies with the potential to discover the bulk of the cluster-scale synchrotron emission in the Universe (Enßlin & Röttgering 2002; Brunetti et al. 2008).

The theoretical picture for γ -ray emission is very complex and modern numerical simulations provide an efficient way to obtain detailed models of non-thermal emission from clusters to compare with present and future observations. Advances in this respect have been recently obtained by including aspects of cosmic-ray physics into cosmological Lagrangian simulations (Pfrommer et al. 2007, 2008), mostly focussing on the acceleration of CRE and CRp at shocks and on the production of secondary electrons from such a CRp population. In this Letter we investigate the non-thermal emission from secondary particles in a Coma-like cluster extracted from a cosmological simulation and, for the first time, compare numerical predictions and observations.

2 THE SIMULATION

We use results from one of the constrained, cosmological MHD simulations presented in Donnert et al. (2009) from which we se-

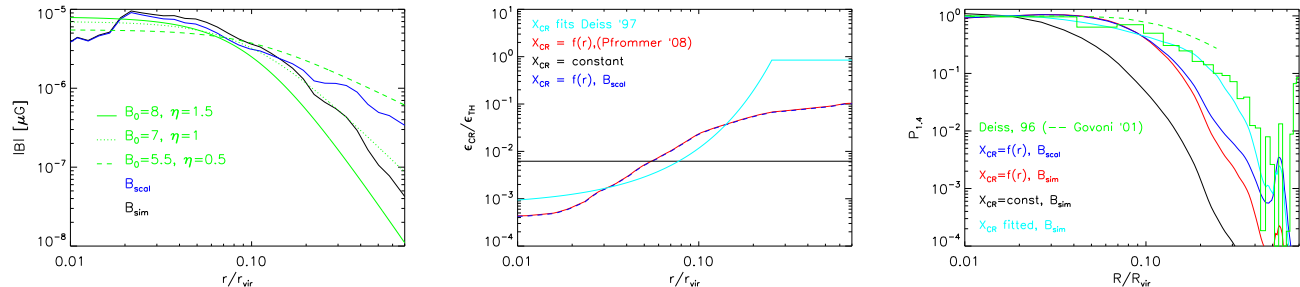


Figure 1. The left panel shows the comparison of the radial profile of the magnetic field in the simulated Coma cluster (black), the scaled version for *Model 3* (blue) and the class models inferred from the observations. The middle panel shows the Energy density fraction of the CRp as function of radius for the different models as indicated in the plot. The right panel shows the radial profile for the radio emission resulting of the different models compared with the observed profile. See text for more details.

lect the simulated counterpart of the Coma cluster. The initial conditions for a constrained realization of the local Universe were the same as used in Mathis et al. (2002). Briefly, the initial conditions were obtained based on the the IRAS 1.2-Jy galaxy survey (see Dolag et al. 2005, for more details). Its density field was smoothed on a scale of 7 Mpc, evolved back in time to $z = 50$ using the Zel-dovich approximation and used as an Gaussian constraint (Hoffman & Ribak 1991) for an otherwise random realization of a Λ CDM cosmology ($\Omega_M = 0.3$, $\Lambda = 0.7$, $h = 0.7$). The IRAS observations constrain a volume of ≈ 115 Mpc centered on the Milky Way. In the evolved density field, many locally observed galaxy clusters can be identified by position and mass. The Coma cluster in particular can be clearly identified by its global properties and gives an excellent match to the observed SZ decrement, especially in the non-radiative simulations used in this Letter (Dolag et al. 2005). The similarity in morphology of the simulated and observed Coma cluster is coincidental, as this structure is far below the constraints originally imposed by the IRAS galaxy distribution. The original initial conditions were extended to include gas by splitting dark matter particles into gas and dark matter, obtaining particle of masses $6.9 \times 10^8 M_\odot$ and $4.4 \times 10^9 M_\odot$ respectively. The gravitational softening length was set to 10 kpc.

Our MHD simulation follow the magnetic field through the turbulent amplification driven by the structure formation process. For the magnetic seed fields a semi-analytic model for galactic winds was used. Here we used the result of the *0.1 Dipole* simulation (Donnert et al. 2009), which gives a reasonable match to the observed magnetic field in the Coma cluster. The left panel of figure 1 compares the magnetic field profile predicted for the Coma cluster from our simulations with models that best reproduce the Rotation Measure observed in five extended sources within the Coma cluster (preliminary results from Bonafede et al. 2009, Bonafede et al. in prep) with a magnetic field radial profile : $\langle B(r) \rangle = B_0 \left[\frac{n_{\text{gas}}(r)}{n_0} \right]^\eta$ and η in the range [0.5 -1.5]. Our simulations are in good agreement with a more centrally peaked profile (e.g. $\eta \approx 1.0$). This profile gives an average magnetic field over the central Mpc^3 of $\sim 1.9 \mu\text{G}$, which is consistent with the equipartition estimate derived from the radio halo emission (Thierbach et al. 2003).

3 SECONDARY ELECTRONS IN GALAXY CLUSTERS

The origin of Mpc-scale radio emission in galaxy clusters is still not fully understood. Extended and fairly regular diffuse synchrotron

emission may be produced by secondary electrons injected during proton-proton collisions, since the parent relativistic protons can diffuse on large scales (e.g. hadronic or secondary models; Denison (1980); Blasi & Colafrancesco (1999)). Alternative models assume relativistic electrons re-accelerated in-situ by MHD turbulence generated in the ICM during cluster-cluster mergers (e.g. re-acceleration models; Brunetti et al. (2001); Petrosian (2001)).

In this letter we focus on hadronic models that can be implemented in present simulations. The spectrum of CRp was taken to be a power law, $N(E) = K_p E^{-\alpha_p}$, and the spectrum of the secondary electrons resulting from p-p collisions was calculated under stationary conditions considering synchrotron and inverse Compton losses (Brunetti & Blasi 2005, and ref. therein). Following Dolag & Enßlin (2000) we adopted the slope of the spectral index of the Coma halo, $\alpha = 1.25$, obtain with $\alpha_p = 2.6$ for the hadronic models (this also accounts for the logarithmic increase of the p-p cross-section with proton energy). Such CRp collisions also produce γ -rays from the decay of secondary neutral-pions, which are a direct measure of the CRp and of the unavoidable secondary electron injection process into the ICM. We calculate the γ -ray flux from our simulated Coma cluster by adopting $\alpha_p = 2.6$ and the formalism described in Pfrommer & Enßlin (2004).

The spatial distribution of CRp in our MHD simulations is a free parameter, so we follow four approaches chosen to encompass a range suggested by theoretical and observational findings, but restricting to large magnetic fields in the ICM that provide the most favourable case for hadronic models. In *Model 1* we assume that the energy density of the CR protons is a constant fraction of the thermal energy density of the ICM. In *Model 2* we adopt a radius-dependent ratio between CRp and thermal energy density following results from cosmological simulations of CRp acceleration at structure formation shocks by Pfrommer et al. (2007). In both these models, we use the magnetic field strength and spatial distribution from our MHD simulations of the Coma cluster. In *Model 3* we adopt the radius-dependent energy density of CRp as in *Model 2* and an artificial magnetic field by assuming a radial scaling of the field strength in the form $B \propto \sqrt{\rho}$ within the radio emitting region (Figure 1). In the last model, *Model 4*, we used the magnetic field from our MHD simulations, but leave the radial profile of the CRp energy density in the simulated cluster free to vary to match the synchrotron brightness profile measured for the Coma radio halo; in this case we limit the CRp energy density so that it stays smaller than the thermal energy density of the ICM.

For all the models the overall normalization of the CRp energy

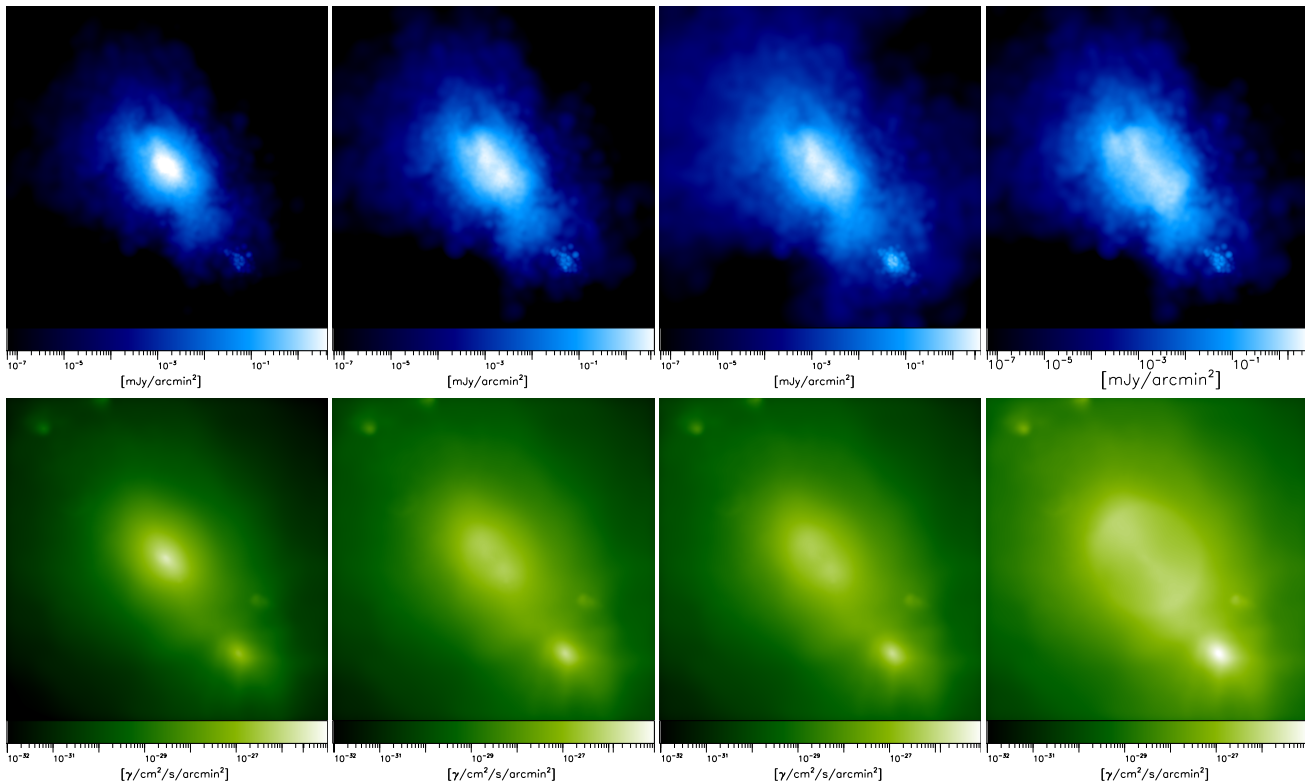


Figure 2. Synthetic radio maps of the simulated Coma cluster (4 Mpc a side). Upper panels are synchrotron maps at 1.4 GHz, lower panels are γ -ray maps at $E_\gamma > 100$ GeV. The four models displayed from left to right are: constant CRp energy fraction (*Model 1*), scaled CRp energy fraction (*Model 2*), scaled magnetic field (*Model 3*) and fitted CRp energy fraction (*Model 4*). The overall normalization of the CRp energy fraction is chosen to match the observed total radio luminosity of Coma.

density is chosen to match the observed radio luminosity of the Coma radio halo at 1.4 GHz, 7.76×10^{23} W/Hz (Deiss et al. 1997).

4 THE RADIO HALO OF COMA

The Coma cluster hosts the prototype of giant radio halos (eg. Giovannini et al. 1993), and in this section we compare the radio properties from the simulated Coma cluster with the observed ones. We calculate simulated radio images by using a map-making algorithm (Dolag et al. 2005), that allows us to project the predicted emission of every SPH particle along the line of sight, considering an integration depth of ± 4 Mpc around the center of the simulated Coma cluster. The resulting images of radio emission for our models are shown in the upper panels of Figure 2.

4.1 Radial profile and cosmic ray energy budget

The radial distributions of the fraction between the energy density of CRp and that of the thermal gas for *Models 1–4* are reported in the central panel of Figure 1. Provided that the magnetic field strength in the cluster-central regions is sufficiently large (i.e. $> 5 \mu\text{G}$, as in our cases), *Models 1–3* generate enough synchrotron luminosity at 1.4 GHz to match that of the Coma halo with reasonable requests in terms of energy density in the CRp (about 1 to 10 % of that of the thermal gas). However, a drawback of hadronic models discussed in the literature is that the radial distribution of the synchrotron emission generated from secondary electrons is expected to be much steeper than that observed in radio halos, with

most of the radio luminosity generated in the cluster-core region (e.g. Brunetti 2004).

The right panel of Figure 1 shows a comparison of the simulated and observed radial profile of the radio emission from the Coma cluster. In line with previous simulations (Dolag & Enßlin 2000) and analytical expectations (e.g. Brunetti 2004) we find that assuming CRp contain a constant fraction of the energy density of the thermal pool (*Model 1*) a profile is produced that is far too steep. Flatter radial profiles of the radio emission, and thus fairly extended radio halos, are generated only by *Models 2* and *3*, yet the expected radio brightness at 0.5–1 Mpc distance from the cluster-center is still > 10 times fainter than that observed in the Coma halo. This picture also arises from the point-to-point scatter plot between radio surface brightness and the X-ray brightness from thermal emission (left panel in figure 3); the solid line is the observed correlation obtained by Govoni et al. (2001).

To reproduce the radial profile as measured at 1.4 GHz by Deiss et al. (1997) out to 0.5–1 Mpc distance, in *Model 4* we allow the energy density of CRp to vary with distance from the cluster center. The resulting radial distribution of the amount of energy in CRp relative to that of the thermal pool is shown in the central panel of Figure 1 and highlights an expected energetic problem of hadronic models: to considerably increase the synchrotron emissivity at large distance from cluster center, where the generation of secondary particles is inefficient due to the small number density of (target) thermal protons, a secondary model requires that the energy density of CRp be extremely large, comparable with (or even larger than) that of the thermal pool. Considering the profile measured with high sensitivity by Westerbork observations at 330 MHz (green, dashed

Mission Model	Veritas (diffuse) (> 0.1TeV)	($r < 1.3$ Mpc) (> 0.1TeV)	Egret (> 0.1GeV)
observed	$< 2.0 \times 10^{-12}$	—	$< 3.8 \times 10^{-8}$
<i>Model1</i>	6.3×10^{-14}	6.6×10^{-14}	1.1×10^{-9}
<i>Model2</i>	6.3×10^{-14}	7.8×10^{-14}	1.2×10^{-9}
<i>Model3</i>	6.4×10^{-14}	8.0×10^{-14}	1.3×10^{-9}
<i>Model4</i>	1.6×10^{-13}	3.7×10^{-13}	6.0×10^{-9}

Table 1. Expected limits of γ -ray emission from the simulated Coma cluster in $\gamma/s/cm^2$, excluding the substructure on the lower right. For the three models of CR distribution we show the limits in energy ranges, corresponding to recent experiments.

line in the right panel of figure 1, Govoni et al. 2001) makes this point even more problematic.

4.2 The Spectrum

The radio spectrum of the Coma halo shows a steepening at higher frequencies (Thierbach et al. 2003) that has been interpreted as a signature of stochastic reacceleration of the emitting electrons (Schlickeiser et al. 1987; Brunetti et al. 2001). On the other hand, it has also been argued that the steepening is due to incorrect estimation of the flux of the radio halo at the highest frequencies due to the Sunyaev-Zeldovich (SZ) decrement (e.g. Enßlin 2002). The latter results in a flux reduction of the cosmic microwave background photons in the cluster region by Compton scattering with the cluster-thermal electrons, which diminishes the radio flux at higher frequencies, although other authors conclude that this is not sufficient to explain the spectral steepening in the Coma halo (Reimer et al. 2004; Brunetti 2004).

Our numerical simulations can be used to investigate SZ-decrement effect on the synchrotron spectral properties. Figure 3 (central panel) shows the radio and inverse Compton spectrum from the SZ effect inside the cluster gas. The red line is the prediction of the total flux from our models, where the SZ signal is extracted from the region of the radio halo at 1.4 GHz, ≈ 500 kpc in radius. The deviation from a pure power law at higher frequencies is due to the SZ flux decrement (the dotted line marks the corresponding power law with $\nu^{1.25}$), while the flattening at lower frequencies is due to the energy-dependent cross-section of p-p collisions. We plot the absolute of the IC flux, although it corresponds to negative flux at frequencies smaller than $\approx 2 \times 10^5$ MHz. In black we show observations from Thierbach et al. (2003) and Battistelli et al. (2002) of the Coma cluster in the radio and microwave band, respectively. We also evaluated the fluxes integrated over the relevant sizes according to the individual observations (red symbols). The observed shape of the radio spectrum, with the steepening at 2×10^3 MHz, cannot be explained by our secondary models, even including the SZ decrement for these frequencies, although the simulated SZ signal almost perfectly fits observations in the microwave regime. The blue dashed line shows the inverse Compton decrement, assuming an isothermal beta model for the thermal gas of Coma with emission region of 5 Mpc radius (as done in Enßlin (2002)), which would be needed to cause the steepening at 5 GHz. This size is about one order of magnitude more extended than the radio emission. Additionally we show in green the expected spectrum from a stochastic electron-acceleration model (Schlickeiser et al. 1987).

5 γ -RAY SPECTRUM AND LIMITS

Maps of the predicted γ -ray emission of our simulated Coma cluster are shown in the lower panels of Figure 2. In the right panel of Figure 3 we show the differential and integral γ -ray flux as function of energy of the photons. Here we also included the observed limits from VERITAS and EGRET (Reimer et al. 2003; Perkins 2008), see Table 1.

We find that the γ -ray emission produced in the case of *Model 4*, to allow a reasonable match with the Deiss et al. profile of the Coma halo (at least at < 0.7 -1 Mpc distance from cluster center), is a factor ~ 6 below present upper limits. As well, matching the radial profile of the Coma halo as measured by high sensitivity observations at 330 MHz would require an even larger energy budget of CRp with respect to that in *Model 4* and consequently a larger γ -ray emission. Thus as soon as future γ -ray observations will reach sensitivities slightly deeper than present upper limits they will allow complementary tests to the hadronic origin of the radio emitting electrons in the Coma cluster. For instance, the expected sensitivity of the Fermi Gamma Ray Telescope will be sufficient to constrain *Model 4*.

6 CONCLUSIONS

Based on a constrained, cosmological MHD simulation of the local universe we investigated the predicted properties of the radio halo of the Coma cluster within the framework of the hadronic model. We follow four approaches, chosen to span the reasonable range suggested by theoretical and observational findings, and focusing on the case of high magnetic field values that represents the most favorable way for hadronic models.

Our main conclusions are:

- In agreement with previous findings, hadronic models may produce the synchrotron radio luminosity of the Coma halo with energy densities of CRp between 1–10% of the thermal ICM. However the radial brightness profile of the generated synchrotron emission is much steeper than seen in observations of the Coma halo, consequently the simulated radio halos come out much smaller than the observed one. This also leads to a slope in the thermal X-ray vs. radio brightness point-to-point correlation that is significantly steeper than the observed one.
- The observed flat radial brightness profile and the fairly large extent of the observed radio halo can only be obtained with hadronic models by strongly increasing the CRp energy density outside the core of the cluster. In this case, however, the resulting CRp energy density at ≈ 1 Mpc (e.g. the rim of the observed radio halo) would equal (or exceed) that of the thermal ICM.
- Our simulated Coma cluster matches almost perfectly the observed SZ decrement. But this SZ decrement is still not enough to explain the spectral steepening observed in the spectrum of the radio halo at large frequencies; contrary to previous claims in literature.

In summary, we find that the hadronic model is disfavored by current observations of the Coma cluster. In principle the energy problem might be alleviated by if the magnetic field strength were almost constant with cluster radius up to the rim of the observed radio halo (see Pfrommer & Enßlin 2004), however such models are not among the best-fitting ones inferred from present RM observations. At the same time we have shown that hadronic models cannot explain the spectral steepening of the Coma radio halo: regardless of

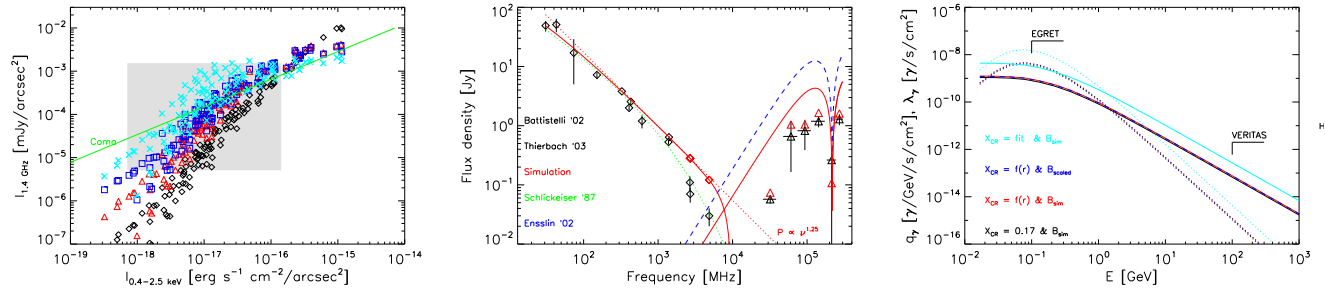


Figure 3. The left panel shows the Radio Flux of the simulated Coma cluster at 1.4 GHz versus X-ray surface brightness. We plot the constant model in black, the model with scaled CRp in red, the one with scaled MF and CRp in blue and the one with fitted CRp in magenta. The solid line is taken from the observations by Govoni et al. (2001). The middle panel shows the observed spectrum of the Coma cluster (synchrotron emission: black diamonds, Thierbach et al. (2003); inverse Compton: black triangles, Battistelli et al. (2002)). Red lines are from the simulation and the red symbols are evaluated within the same aperture as the according observations. See text for more details. The right panel shows the expected γ -ray spectrum from the simulated Coma cluster for the our different models for the CRp distribution and the integrated γ -ray spectrum (within $r < 1.3$ Mpc) with the current upper limits from EGRET and VERITAS (Reimer et al. 2003; Perkins 2008).

the model assumptions, an SZ effect matching observations produces a negligible SZ decrement at 2.7 and 5 GHz in the region of the halo.

The γ -ray flux generated by the hadronic interaction in case of *Model 4*, which alone matches the observed radial profile is only a factor ~ 6 below the current limits. Considering that in case of lower magnetic fields (and/or assuming the more extended profile of the Coma halo from high sensitivity 330 MHz observations) the expected γ -ray flux should significantly increase, we conclude that incoming γ -ray observations will shortly provide additional constraints to the models.

7 ACKNOWLEDGEMENTS

J. Donnert kindly acknowledges the support of ESF/Astrosim Exchange grant 2065 and thanks the INAF/IRA in Bologna for its hospitality. GB, RC and AB acknowledge partial support from PRIN-INAF2007 and ASI-INAF I/088/06/0.

REFERENCES

- Aharonian F., Akhperjanian A. G., Anton G., Barres de Almeida U., Bazer-Bachi A. R., Becherini Y., Behera B., Bernlöhr K., Boisson C., Bochow A., et al. 2009, *A&A*, 495, 27
- Battistelli E. S., De Petris M., Lamagna L., Melchiorri F., Palladino E., Savini G., Cooray A., Melchiorri A., Rephaeli Y., Shimon M., 2002, *ApJ*, 580, L101
- Blasi P., 2001, *Astroparticle Physics*, 15, 223
- Blasi P., Amato E., Caprioli D., 2007, *MNRAS*, 375, 1471
- Blasi P., Colafrancesco S., 1999, *Astroparticle Physics*, 12, 169
- Bonafede A., Govoni F., Murgia M., Feretti L., Dallacasa D., Giovannini G., Dolag K., Taylor G., 2009, in ‘Magnetic Fields in the Universe II Rev. Mex. Astron. Astrof., Coma
- Brunetti G., 2004, *Journal of Korean Astronomical Society*, 37, 493
- Brunetti G., 2008, *ArXiv* 0810.0692
- Brunetti G., Blasi P., 2005, *MNRAS*, 363, 1173
- Brunetti G., Giacintucci S., Cassano R., Lane W., Dallacasa D., Venturi T., Kassim N. E., Setti G., Cotton W. D., Markevitch M., 2008, *Nature*, 455, 944
- Brunetti G., Lazarian A., 2007, *MNRAS*, 378, 245
- Brunetti G., Setti G., Feretti L., Giovannini G., 2001, *MNRAS*, 320, 365
- Cassano R., 2009, *ArXiv* 0902.2971
- Deiss B. M., Reich W., Lesch H., Wielebinski R., 1997, *A&A*, 321, 55
- Dennison B., 1980, *ApJ*, 239, L93
- Dolag K., Bartelmann M., Lesch H., 2002, *A&A*, 387, 383
- Dolag K., Enßlin T. A., 2000, *A&A*, 362, 151
- Dolag K., Grasso D., Springel V., Tkachev I., 2005, *Journal of Cosmology and Astro-Particle Physics*, 1, 9
- Dolag K., Hansen F. K., Roncarelli M., Moscardini L., 2005, *MNRAS*, 363, 29
- Donnert J., Dolag K., Lesch H., Müller E., 2009, *MNRAS*, 392, 1008
- Enßlin T. A., 2002, *A&A*, 396, L17
- Ensslin T. A., Biermann P. L., Klein U., Kohle S., 1998, *A&A*, 332, 395
- Enßlin T. A., Röttgering H., 2002, *A&A*, 396, 83
- Feretti L., 2003, in Bowyer S., Hwang C.-Y., eds, *Astronomical Society of the Pacific Conference Series Vol. 301 of Astronomical Society of the Pacific Conference Series, Radio Observations of Clusters of Galaxies*. pp 143–+
- Ferrari C., Govoni F., Schindler S., Bykov A. M., Rephaeli Y., 2008, *Space Science Reviews*, 134, 93
- Govoni F., Enßlin T. A., Feretti L., Giovannini G., 2001, *A&A*, 369, 441
- Hoffman Y., Ribak E., 1991, *ApJ*, 380, L5
- Mathis H., Lemson G., Springel V., Kauffmann G., White S. D. M., Eldar A., Dekel A., 2002, *MNRAS*, 333, 739
- Perkins J. S., 2008, in *American Institute of Physics Conference Series Vol. 1085 of American Institute of Physics Conference Series, VERITAS Observations of the Coma Cluster of Galaxies*. pp 569–572
- Petrosian V., 2001, *ApJ*, 557, 560
- Petrosian V., Bykov A., Rephaeli Y., 2008, *Space Science Reviews*, 134, 191
- Pfrommer C., Enßlin T. A., 2004, *A&A*, 413, 17
- Pfrommer C., Enßlin T. A., Springel V., 2008, *MNRAS*, 385, 1211
- Pfrommer C., Enßlin T. A., Springel V., Jubelgas M., Dolag K., 2007, *MNRAS*, 378, 385
- Reimer A., Reimer O., Schlickeiser R., Iyudin A., 2004, *A&A*, 424, 773

Reimer O., Pohl M., Sreekumar P., Mattox J. R., 2003, ApJ, 588,
155

Schlickeiser R., Sievers A., Thiemann H., 1987, A&A, 182, 21

Subramanian K., Shukurov A., Haugen N. E. L., 2006, MNRAS,
366, 1437

Thierbach M., Klein U., Wielebinski R., 2003, A&A, 397, 53